

Identifying an influential spreader from a single seed in complex networks via a message-passing approach

Byungjoon Min¹

IFISC, Instituto de Física Interdisciplinar y Sistemas Complejos (CSIC-UIB), Campus Universitat Illes Balears, E-07122 Palma de Mallorca, Spain e-mail: byungjoon@ifisc.uib-csic.es

Received: date / Revised version: date

Abstract. Identifying the most influential spreaders is one of outstanding problems in physics of complex systems. So far, many approaches have attempted to rank the influence of nodes but there is still the lack of accuracy to single out influential spreaders. Here, we directly tackle the problem of finding important spreaders by solving analytically the expected size of epidemic outbreaks when spreading originates from a single seed. We derive and validate a theory for calculating the size of epidemic outbreaks with a single seed using a message-passing approach. In addition, we find that the probability to occur epidemic outbreaks is highly dependent on the location of the seed but the size of epidemic outbreaks once it occurs is insensitive to the seed. We also show that our approach can be successfully adapted into weighted networks.

PACS. 05.70.Ln Nonequilibrium and irreversible thermodynamics – 89.65.-s Social and economic systems – 89.75.Hc Networks and genealogical trees

1 Introduction

The topological location of the origin of spreading dynamics plays an important role in a final configuration of spreading processes [1, 2, 3, 4, 5, 6, 7, 8]. For example, an initial patient from which an epidemic starts to spread influences critically the total number of infected patients [2, 9, 10]. In addition, influential spreaders are required to be targeted for immunization with a high priority to halt epidemic outbreaks or rumor spreading [11, 12, 13, 14, 15]. Searching for the most influential nodes in complex networks has attracted much attention from many disciplines such as physics, complex network science, sociology, and computer science due to its practical application in real-world spreading processes including emerging epidemics and information diffusion [2, 3, 4, 5, 8, 9, 10, 16, 17, 18, 19, 20, 21, 22, 23].

Several centralities in terms of network topology from degree [24] that is the number of neighbors to k -core [25], betweenness centrality [26], and PageRank [27] have been tested for identifying influential spreaders. Even though many methods so far have been proposed to single out influential spreaders, however there are still limitations in their accuracy and applicability because most of them were based on intuition rather than on mathematical background. In addition, while the ranking of nodes' influence would rely on the details of spreading processes such as the probability of transmission, most previous methods do not take into account the processes of spreading dynamics explicitly [2, 9, 10, 18, 19].

In order to overcome these limitations, we directly derive a theory for finding influential spreaders based on a message-passing approach. We compute the expected size of epidemic outbreaks on locally tree-like networks, when an epidemic starts from a single node. We validate our theory with extensive numerical simulations on synthetic and empirical networks with various transmission probabilities. We confirm that our theory can predict accurately the influence of spreaders in complex networks. We also find that the location of an initial spreader affects the probability of epidemic outbreaks but not the average size of epidemic outbreaks once it occurs. In addition, we show that our approach based on message-passing equations can be applied to weighted networks.

2 Theory

We consider the susceptible-infected-recovered (SIR) model as a typical epidemic model [28]. The SIR model is regarded as one of the most simple yet successful models describing irreversible spreading processes. The SIR model consists of three states: susceptible (S), infected (I), and recovered or removed (R). Each infected node is infectious to spread disease to its neighbors on a network with the infection rate β . Independently, each infected node becomes recovered after the recovery time τ . Once recovered, it is not infectious anymore, leading to an irreversible process. Thus, an infected node is able to spread a disease to its neighbors during the recovery time from the moment of

infection. For the sake of simplicity, we assume that the recovery time is sharply distributed, and so its probability distribution $P(\tau)$ is well described by the delta function.

We implement the SIR model on complex networks with a single seed. To be specific, all nodes are initially susceptible except a single infected node i which corresponds to the first patient. An infected node transmits disease to its neighbors with the infection probability β and autonomously recovers with the recovery time τ . Without loss of generality, we set $\langle\tau\rangle = 1$ in our study. These processes proceed until there are no more infected nodes in a system. In the stationary state ($t \rightarrow \infty$), we measure the fraction of recovered nodes ρ_i when epidemic starts with a single seed i , called the prevalence of epidemic outbreaks. The higher prevalence ρ_i is the higher influence of node i is, because higher ρ_i implies that an epidemic initiated by node i brings out larger epidemics in average.

Once we obtain the prevalence of each node ρ_i , we can directly identify influential spreaders based on sorting of ρ_i . However, it is a time-consuming process to obtain ρ_i for every node in a system by numerical simulations because many realizations for every different seed are needed. Thus, we derive a theory for estimating the prevalence for a seed via a message-passing approach. A message-passing approach has also been applied for percolation [29], inferring the origin of spreading [30], optimal immunization [15], optimal deployment of resource [31], and optimal percolation [19, 32]. We use mapping between the epidemic model with the static bond percolation, which is well known for a long time [33, 34, 35]. Then, we reinterpret the message-passing approach for bond percolation as a theory for identifying superspreaders in the epidemic model [9]. In this section, we present the message-passing equations and its interpretation for the SIR model.

We first consider a classical bond percolation problem on complex networks with a size N and link occupation probability T_B . In a percolation process, there can be one giant component \mathcal{G} that is a connected cluster that covers a non-vanishing fraction of a network in the limit $N \rightarrow \infty$ and multiple small components. The giant component appears only if T_B is sufficiently high, i.e., T_B is larger than the percolation threshold. If T_B is less than the threshold, there exist only small components. At the percolation threshold, the giant component appears, showing a typical second-order phase transition between non-percolating and percolating phases.

For the mapping between the bond percolation with SIR model, let us imagine a final configuration of the SIR model in the steady state. In the limit $t \rightarrow \infty$, all nodes in a network are either susceptible or recovered. Note that all infected nodes become eventually recovered. We then define links on which infection occurs as infection links whose probability is given by transmissibility T . The transmissibility is then the probability that an infected node infects its neighbors before it recovers, and therefore $T = 1 - e^{-\beta\tau}$ [35]. The relation between the SIR model and bond percolation is established by correspondence between the transmissibility T in the SIR model and the probability of link occupation in bond per-

colation T_B . Then, the size of epidemic outbreaks in the steady state corresponds to the size of connected component by infection links which is fully determined by the structural property of a final configuration. In the steady state, the epidemic size at a given T corresponds to the size of \mathcal{G} with the same occupation probability T_B in the bond percolation jargon. Thus, a continuous transition between disease-free phase and global epidemic phase at the epidemic threshold is observed, similar with the bond percolation. Based on this mapping, we derive a theory for finding influential nodes in the SIR model, using a message-passing approach developed in percolation theory.

In order to derive the theory for the SIR model, first define H_{ij} as the probability that node j by following a link from node i does not bring out an epidemic outbreak with the transmissibility T . Assuming locally tree-like structures, if neither the link between i and j is infection link nor all the neighbors of node j excluding node i occur an epidemic outbreak, node j does not bring out an epidemic outbreak. Thus, the probability H_{ij} can be obtained by following coupled self-consistency equations [9, 29, 36, 37, 38],

$$H_{ij} = 1 - T + T \prod_{k \in \partial j \setminus i} H_{jk}. \quad (1)$$

where $k \in \partial j \setminus i$ represents a set of neighbors of node j excluding node i . Computing the above self-consistency equations iteratively, H_{ij} converges towards a fixed point. We here concentrate only on locally tree-like structure, but our framework can also be extended for networks with triangles beyond locally tree-like structures [38].

When H_{ij} is obtained, we can calculate the probability P_i that a seed i triggers an epidemic outbreak in terms of H_{ij} as

$$P_i = 1 - \prod_{j \in \partial i} H_{ij}, \quad (2)$$

where $j \in \partial i$ indicates a set of neighbors of node i . When T is less than the epidemic threshold, P_i is zero since there is no global epidemic. In the bond percolation jargon, P_i is the probability that a randomly chosen node i belongs to the giant component \mathcal{G} . Similarly, we can obtain the size of epidemic when it occurs from a seed i by

$$S_i = \frac{1}{N} \left(1 + \sum_{\substack{j=1 \\ j \neq i}}^N P_j \right). \quad (3)$$

Since a node i has to be included in the epidemic outbreak as a seed, we differently treat node i in the summation. After we obtain the probability and size of epidemic outbreaks, we can simply calculate the average prevalence when the epidemic is initiated by a seed i as

$$\rho_i = P_i S_i. \quad (4)$$

In summary, (i) we obtain H_{ij} by calculating iteratively Eq. 1 with a given T , (ii) compute P_i by Eq. 2, S_i by

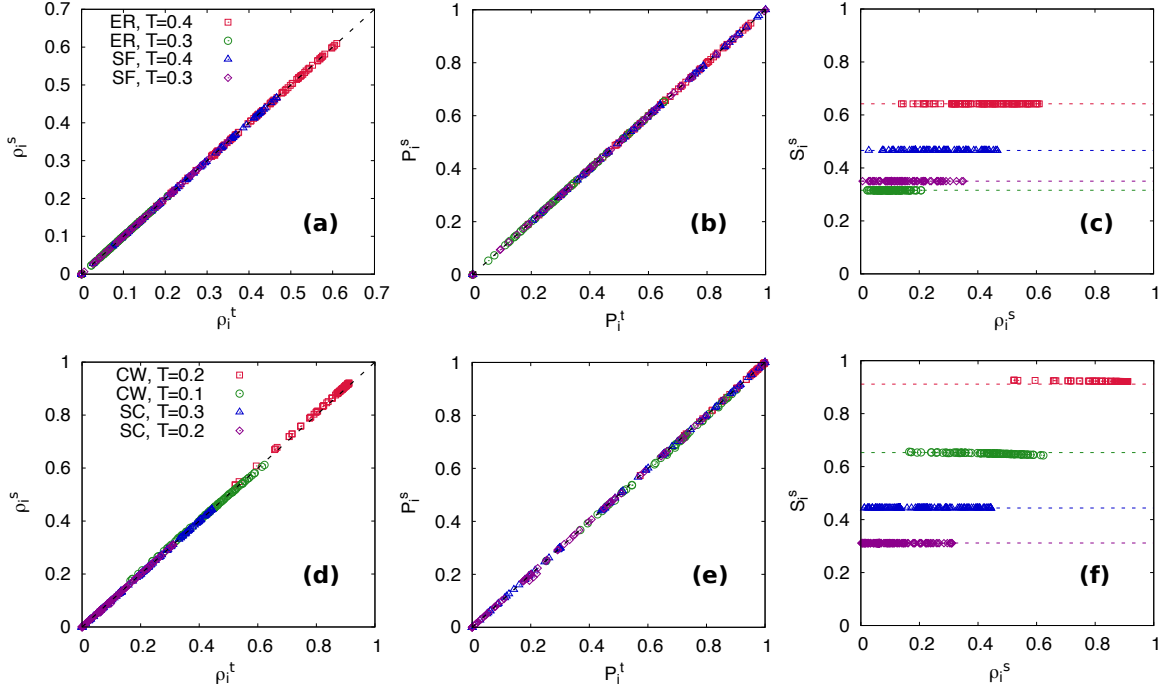


Fig. 1. Scatter plot of (a) prevalence ρ_i , (b) probability P_i , and (c) size S_i of epidemics initiated from node i obtained by theory and numerical simulations for ER and SF networks with $N = 10^5$ with different transmissibility. The same plot for the empirical networks, CW and SC, are shown in (d-f). Dashed lines in (c) and (f) represent average epidemic size obtained by theory as $S = \frac{1}{N} \sum_i^N P_i$. The theory is in perfect agreement with the numerical simulations for both random and empirical networks.

Eq. 3, and ρ_i by Eq. 4 for different seed selection, and (iii) identify superspreaders based on sorting the prevalence of each node ρ_i .

Our theory provides not only the ranking of influential spreaders but also intriguing perspectives on finding superspreaders. First, the size of epidemic outbreaks is insensitive to the location of an initial seed once the spread reaches global epidemics. Thus the difference in the influence for different seeds is mainly caused by the epidemic probability of each seed. Second, the ranking of influential spreaders is not fully determined by only the topological location of seed but can vary depending on the parameters of spreading processes and details of spreading models [39]. Therefore, it would be misleading if one attempts to find a universal ranking of influential spreaders solely relying on network structures ignoring dynamical properties of spreading processes as reported in [39].

3 Results

We first test our theory with numerical simulations on Erdős-Rényi (ER) and scale-free (SF) networks with $N = 10^5$ which respectively represent random graphs with a homogeneous and heterogeneous degree distribution. For building ER networks, we randomly choose a pair of nodes and connect them unless they are already connected. We repeat this step until the mean degree $\langle k \rangle$ reaches the desired value. In our study, we set $\langle k \rangle = 4$.

For building SF networks, we use static scale-free network model [40]. In the model, each node i has its inherent weight ω_i given by $\omega_i = i^{-\mu} / \sum_{j=1}^N j^{-\mu}$, where μ is a constant, $0 < \mu < 1$, which determines the degree exponent. We choose a pair of nodes, say i and j independently following the probability w_i and w_j respectively, and connect them unless they are already connected. We repeat this step until the mean degree $\langle k \rangle$ reaches the desired value which is $\langle k \rangle = 2$ in our study. The degree distribution of the resulting network is asymptotically scale-free with the decaying tail $k^{-\gamma}$ with the degree exponent $\gamma = (\mu + 1)/\mu$, i.e., $\gamma = 2.5$ in our study.

On the resulting network, we perform the SIR process with every single seed i . The prevalence with seed i is obtained, averaged over 10^4 independent runs. The prevalence obtained by the theory ρ_i^t and numerical simulation ρ_i^s are shown together in Fig. 1(a). Our theory exhibits perfect agreement with the numerical results. Pearson correlation coefficient between ρ_i for the theory and simulation is larger than 0.99 for all tested infection rate and network structures. Note that non-backtracking centrality corresponds to the limit $H_{ij} \rightarrow 1$ where T is at an epidemic threshold. Thus, non-backtracking centrality can predict the influence of spreaders reliably at the epidemic threshold as a special case of our theory near the epidemic threshold [9, 41].

We also validate our theory for the SIR model on top of empirical contact networks. In order to reconstruct real-world networks, we use contacts in a workplace net-

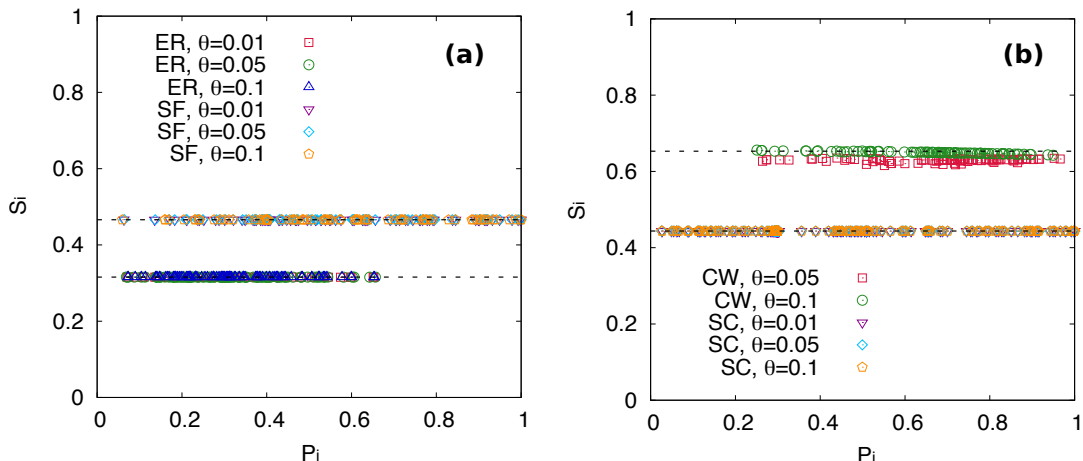


Fig. 2. (a) Scatter plot of size S_i of epidemics initiated from node i with respect to probability of epidemics P_i obtained by the numerical simulations for ER ($T = 0.3$) and SF ($T = 0.4$) networks with $N = 10^5$ and different threshold $\theta = 0.01, 0.5, 0.1$. (b) The same plot for the empirical networks, CW ($T = 0.1$) and SC ($T = 0.3$), with $\theta = 0.01, 0.5, 0.1$. For the CW network, the result with $\theta = 0.01$ is discarded since the network size is less than 100. Dashed lines represent average epidemic size obtained by theory.

work (CW) from face-to-face contact patterns between individuals in an office building in France [42] and a sexual contact network (SC) containing the information of sexual activity gathered from a web community of internet-mediated prostitution in Brazil [43]. Both networks contain the moment of contacts between individuals. Note that both networks are far different from random networks because the CW has a strong modular structure based on the organization of the offices in departments and the SC is a completely bipartite network. Therefore, these networks are suitable examples to evaluate how well the theory works beyond random networks. As shown in Fig. 1(d), the theory predicts the final fraction of epidemic outbreaks accurately for the empirical networks. Correlation coefficient between the theory and numerical simulation reaches more than 0.99, indicating perfect agreement between them.

Beyond the agreement in the prevalence between the theory and numerical results, we decompose ρ_i into the probability P_i and size S_i of epidemics. In numerical simulation, we define global epidemics when more than 10 % of nodes in a network ultimately are infected. We compute numerically the probability P_i of epidemic outbreaks as the frequency of global epidemics out of all trials and the size S_i of outbreaks when global epidemic occurs. We compare the probability and size obtained by the theory and numerical results for ER, SF, CW, and SC networks in Fig. 1. We find that our theory reliably predicts the probability and size of epidemic outbreaks. We also find that while the probability P_i shows different values for different initial seeds, the size S_i is almost constant and insensitive to seed location. Thus, the epidemic size once global epidemic occurs S_i is independent to ρ_i . This result implies that the location of seed affects the probability to bring out a global epidemic but not the size of an epidemic once it occurs.

We also confirm that the numerical results are highly robust for the different definition of the global epidemic. Specifically, we check the size of epidemics S_i when the fraction of infected nodes exceeds a threshold value θ , 1, 5, and 10 % out of all nodes (Fig. 2). We find that the different threshold values θ do not produce notable difference at all. The irrelevance of the seed location to S_i can be understood if we recall the mapping between the bond percolation and the SIR model. The epidemic size S_i from a single seed can be regarded as the average size of giant component including node i in the perspective on the bond percolation. Therefore, S_i is rather insensitive to the topological location of a seed i . In contrast, P_i strongly relies on the location of a seed since it can be interpreted as the probability that a randomly chosen node belongs to the giant component in the bond percolation.

Next, we generalize our theory for weighted networks, assigned different transmissibility for each link. Despite ubiquity of heterogeneity in link weights, most centralities of complex networks have aimed to single out influential spreaders on unweighted networks except a few studies [44, 45]. We here modify the theory for unweighted networks by introducing a different transmissibility T_{ij} for each link. Substituting T_{ij} into T in Eq. 1, we can obtain the probability H_{ij} that node j arrived through a link from node i does not bring out epidemic outbreaks on weighted networks by

$$H_{ij} = 1 - T_{ij} + T_{ij} \prod_{k \in j \setminus i} H_{jk}. \quad (5)$$

After getting H_{ij} , the probability that a seed node i produces epidemics and the average size of epidemics when a global epidemic occurs can be computed by using the same equations for unweighted networks.

We test the theory for weighted networks with CW and SC networks. Both datasets contain the number of

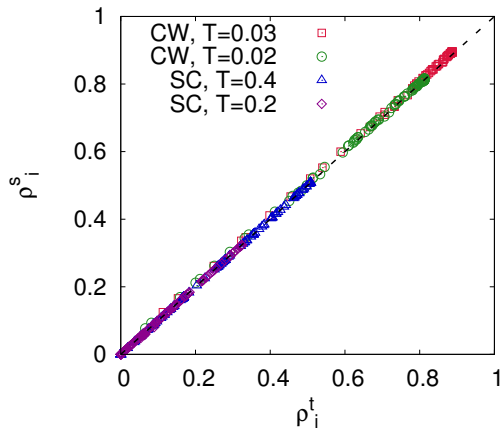


Fig. 3. Scatter plot of the prevalence for theory ρ_i^t and numerical simulations ρ_i^s on top of weighted networks obtained from CW and SC networks. The theory is in good agreement with the numerical simulations.

contacts between two individuals, ν_{ij} . We define the transmissibility between individuals as $T_{ij} = 1 - e^{-\beta\nu_{ij}\tau}$. The transmissibility increases with increasing ν_{ij} , and T_{ij} becomes unity in the limit $\nu_{ij} \rightarrow \infty$. When all $\nu_{ij} = 1$, it is reduced into an unweighted network. Taking into account the weights of each link, we calculate the prevalence of epidemic outbreaks for each seed on CW and SC networks. As shown in Fig. 3, we find that our theory for weighted networks is in well agreement with the numerical simulations for the prevalence of outbreaks. Thus, we confirm that our method based on message-passing equations can also predict reliably the influential spreaders in weighted networks.

While our theory is reliable for the identification of an influential spreader on locally tree-like networks, it has some limitations. First, the theory might break down for networks with many short loops such as spatial networks [46] since they violate the assumption of locally tree-like structures. Second, our method does not guarantee its validity for finding a set of multiple influential seeds that can spread disease or information to the largest part of a network. Note that the problem of identifying multiple influential spreaders is far different and difficult than that of a single spreader because infected nodes by different seeds can be largely overlapped [8, 47].

4 Discussion

In this study, we propose an accurate method for identifying the most influential spreaders for both unweighted and weighted networks via message-passing equations. Our theory is based on the exact mapping between the SIR model and bond percolation, and exact for sparse networks with a locally tree-like structure. We show that the theory is in perfect agreement with numerical calculations, and can outperform previous approaches in terms of accuracy. Furthermore, we find that the location of seed affects the

probability of epidemic outbreaks but not the size of outbreaks, which is not well reported in previous study. Our study can shed light on the identification of the most important spreaders with a single seed in complex networks theoretically and practically, for instance for viral marketing, efficient immunization strategy, and identifying the most influential agents in society.

We thank M. San Miguel and R. Gallotti for useful discussions. We also thank A. Y. Lokhov for suggesting references related. This work was supported by the Spanish Ministry MINEiCO and FEDER (EU) under the project ESOTECOS (FIS2015-63628-C2-2-R).

Author contribution statement

B. M. conceived the study, performed the research, analyzed data, and wrote the paper.

References

1. R. Pastor-Satorras, C. Castellano, P. van Mieghem, and A. Vespignani, *Rev. Mod. Phys.* **87**, 925-979 (2015).
2. M. Kitsak, L. K. Gallos, S. Havlin, F. Liljeros, L. Muchnik, H. E. Stanley, and H. A. Makse, *Nature Phys.* **6**, 888 (2010).
3. C. Castellano and R. Pastor-Satorras, *Sci. Rep.* **2**, 371 (2012).
4. J. Borge-Holthoefer and Y. Moreno, *Phys. Rev. E* **85**, 026116 (2012).
5. K. Klemm, M. Á. Serrano, V. M. Eguíluz, and M. San Miguel, *Sci. Rep.* **2**, 292 (2012).
6. Y. Y. Liu, J. J. Slotine, and A.-L. Barabási, *Nature* **473**, 7346 (2011).
7. J. Gao, Y. Y. Liu, R. M. D'Souza, and A.-L. Barabási, *Nat. Comm.* **5**, 5415 (2014).
8. S. Pei and H. A. Makse, *J. Stat. Mech.* **12**, 12002 (2013).
9. F. Radicchi and C. Castellano, *Phys. Rev. E* **93**, 062314 (2016).
10. L. Lü, T. Zhou, Q. M. Zhan, and H. E. Stanley, *Nat. Comm.* **7**, 10168 (2016).
11. R. Cohen, S. Havlin, and D. Ben-Avraham, *Phys. Rev. Lett.* **91**, 247901 (2003).
12. P. Holme, *EPL (Europhys. Lett)* **68**, 908 (2004).
13. Y. Chen, G. Paul, S. Havlin, F. Liljeros, and H. E. Stanley, *Phys. Rev. Lett.* **101**, 058701 (2008).
14. N. Masuda, *New J. Phys.* **11**, 123018 (2009).
15. F. Altarelli, A. Braunstein, L. Dall'Asta, J. R. Wakeling, and R. Zecchina, *Phys. Rev. X* **44**, 021024 (2014).
16. F. Bauer and J. T. Lizier, *EPL (Europhys. Lett)* **99**, 68007 (2012).
17. S. Pei, L. Muchnik, J. S. Jr. Andrade, Z. Zheng, and H. A. Makse, *Sci. Rep.* **4**, 5547 (2014).
18. B. Min, F. Liljeros, and H. A. Makse, *PLoS ONE* **10**, e0136831 (2015).
19. F. Morone and H. A. Makse, *Nature* **542**, 65 (2015).
20. F. Morone, B. Min, L. Bo, R. Mari, and H. A. Makse, *Sci. Rep.* **6**, 30062 (2016).

21. F. Morone, K. Roth, B. Min, H. E. Stanley, and H. A. Makse, *Proc. Natl. Sci. Acad.* **114**, 3849-3854 (2017).
22. Y. Liu, M. Tang, T. Zhou, and Y. Do, *Physica A* **452**, 289 (2016).
23. F. D. Malliaros, M. E. G. Rossi, and M. Vazirgiannis, *Sci. Rep.* **6**, 19307 (2016).
24. R. Albert, H. Jeong, and A.-L. Barabási, *Nature* **406**, 378 (2000).
25. S. N. Dorogovtsev, A. V. Goltsev, and J. F. F. Mendes, *Phys. Rev. Lett.* **96**, 040601 (2006).
26. L. C. Freeman, *Soc. Netw.* **1**, 215-239 (1979).
27. S. Brin and L. Page, *Comput. Networks ISDN* **30**, 107-117 (1998).
28. W. O. Kermack and A. G. McKendrick, *Proc. Royal Soc. London A* **115**, 700 (1927).
29. B. Karrer, M. E. J. Newman, and L. Zdeborová, *Phys. Rev. Lett.* **113**, 208702 (2014).
30. A. Y. Lokhov, M. Mézard, H. Ohta, and L. Zdeborová, *Phys. Rev. E* **90**, 012801 (2014).
31. A. Y. Lokhov and D. Saad, *Proc. Natl. Acad. Sci.* **114**, E8138 (2017).
32. A. Braunstein, L. Dall'Asta, G. Semerjian, and L. Zdeborová, *Proc. Natl. Acad. Sci.* **113**, 12368 (2016).
33. P. Grassberger, *Math. Biosc.* **63**, 157 (1983).
34. J. L. Cardy and P. Grassberger, *J. Phys. A* **18**, L267 (1985).
35. M. E. J. Newman, *Phys. Rev. E* **66**, 016128 (2002).
36. B. Karrer and M. E. J. Newman, *Phys. Rev. E* **82**, 016101 (2010).
37. A. Y. Lokhov, M. Mézard, and L. Zdeborová, *Phys. Rev. E* **91**, 012811 (2015).
38. F. Radicchi and C. Castellano, *Phys. Rev. E* **93**, 030302 (2016).
39. F. Radicchi and C. Castellano, *Phys. Rev. E* **95**, 012318 (2017).
40. K.-I. Goh, B. Kahng, and D. Kim, *Phys. Rev. Lett.* **87**, 278701 (2001).
41. T. Martin, X. Zhang, and M. E. J. Newman, *Phys. Rev. E* **90**, 052808 (2014).
42. M. Génois *et al.*, *Netw. Sci.* **3**, 326 (2015).
43. L. E. C. Rocha, F. Liljeros, and P. Holme, *Proc. Natl. Acad. Sci. USA* **107**, 5706-5711 (2010).
44. A. Garas, F. Schweitzer, and S. Havlin, *New J. Phys.* **14**, 083030 (2012).
45. C. Gao, D. Wei, Y. Hi, S. Mahadevan, and Y. Deng, *Physica A* **392**, 5490 (2013).
46. M. Barthélemy, *Phys. Rep.* **499**, 1-101 (2011).
47. D. Kempe, J. Kleinberg, É Tardos, *Proceedings of the ninth ACM SIGKDD international conference on Knowledge discovery and data mining*, 137-146 (2003).